

# Hydrogen Leak Detection Using Laser-Induced Breakdown Spectroscopy

A. J. BALL, V. HOHREITER, and D. W. HAHN\*

Department of Mechanical and Aerospace Engineering, University of Florida, Gainesville, Florida 32611

Laser-induced breakdown spectroscopy (LIBS) is investigated as a technique for real-time monitoring of hydrogen gas. Two methodologies were examined: The use of a 100 mJ laser pulse to create a laser-induced breakdown directly in a sample gas stream, and the use of a 55 mJ laser pulse to create a laser-induced plasma on a solid substrate surface, with the expanding plasma sampling the gas stream. Various metals were analyzed as candidate substrate surfaces, including aluminum, copper, molybdenum, stainless steel, titanium, and tungsten. Stainless steel was selected, and a detailed analysis of hydrogen detection in binary mixtures of nitrogen and hydrogen at atmospheric pressure was performed. Both the gaseous plasma and the plasma initiated on the stainless steel surface generated comparable hydrogen emission signals, using the 656.28 H $\alpha$  emission line, and exhibited excellent signal linearity. The limit of detection is about 20 ppm (mass) as determined for both methodologies, with the solid-initiated plasma yielding a slightly better value. Overall, LIBS is concluded to be a viable candidate for hydrogen sensing, offering a combination of high sensitivity with a technique that is well suited to implementation in field environments.

Index Headings: Laser-induced breakdown spectroscopy; LIBS; Hydrogen; Plasma; Atomic emission.

## INTRODUCTION

Hydrogen is a highly flammable gas at ambient conditions, with a flammability range from about 4 to 75% by volume in ambient air. Therefore, leaks associated with hydrogen storage and handling processes must be considered to ensure overall safety. In particular, hydrogen is a primary fuel in the U.S. space shuttle program and is being widely promoted for use with fuel cells and other non-hydrocarbon-based power cycles. As experts discuss an expanding hydrogen distribution infrastructure, associated safety issues must be a key element. As an example, the system complexity and very large volumes of liquid hydrogen associated with the space shuttle program necessitate a detailed set of procedures and equipment to prevent leaks and potentially catastrophic accidents. Initially, helium is used to determine the integrity of the storage and fuel tanks followed by continuous monitoring throughout the system during operation. To date, all monitoring systems have been based on sampling at various locations around the orbiter and using mass spectrometry to detect the presence of leaking hydrogen or oxygen.<sup>1</sup> While mass spectrometry is a sensitive analytical technique, widespread monitoring of hydrogen under field conditions, such as during shuttle operations or at hydrogen distribution centers, could benefit from additional sensor technologies that may offer potential advantages in system size, cost, robustness, and reduced maintenance requirements. This paper examines

the feasibility of using the technique of laser-induced breakdown spectroscopy (LIBS) as a real-time sensor for hydrogen.

Laser-induced breakdown spectroscopy is a form of atomic emission spectroscopy in which a laser is used to generate a plasma via breakdown of the sample material, either in a gaseous state or directly on a solid surface. The high-temperature, energetic plasma results in a dissociation of molecules and subsequent breakdown of the analytical sample into atoms, ions, and free electrons. The plasma may initially be created on a surface because the initial energy requirements to generate breakdown are less as compared to a purely gaseous sample due to the higher electron densities and electron mobility in the solid state. Plasmas generated against solid surfaces expand on a timescale of nanoseconds, subsequently enveloping a sample of the gas phase above the original surface. Following plasma generation, examination of the optical emission, notably atomic emission lines of the plasma's constituent elements, forms the basis of LIBS as an analytical technique. As typically implemented, LIBS requires a relatively simple apparatus consisting of a pulsed laser, sample chamber, spectrometer and array detector, and associated optics. Algorithms have been developed to allow for real-time evaluation of chemical species, producing almost instantaneous results.

The LIBS technique has been reported in a number of studies, including use for spectroscopic analysis of a range of gaseous species such as halogens,<sup>2-4</sup> and analysis of oxygen, nitrogen, carbon monoxide, and carbon dioxide systems.<sup>5-7</sup> Overall, laser-induced breakdown spectroscopy has been shown as a promising technique for the detection of species such as fluorine, chlorine, sulfur, and carbon with applications in chemical weapons monitoring.<sup>2</sup> LIBS offers the possibility of non-interactive, automated sampling in which detection limits can be optimized temporally. LIBS-based detection limits are usually comparable with other plasma spectroscopic methods such as microwave-induced plasma emission spectroscopy and inductively coupled plasma emission spectroscopy, with the added benefit of allowing for *in situ* measurement. LIBS also has been demonstrated to be a promising tool in monitoring gaseous fluoride emissions that are relevant to the aluminum processing industry<sup>4</sup> and for the detection of combustion species, namely, on-line engine equivalence ratio measurements.<sup>8</sup> In the realm of fire suppression and pollution monitoring, LIBS has been examined as a viable detection technique for halon alternatives with demonstrated detection limits in the parts per million.<sup>3</sup> While these applications examine the practicality of LIBS as a gaseous species detection scheme, there has been no investigation of LIBS as a practical scheme

Received 5 June 2004; accepted 22 November 2004.

\* Author to whom correspondence should be sent.

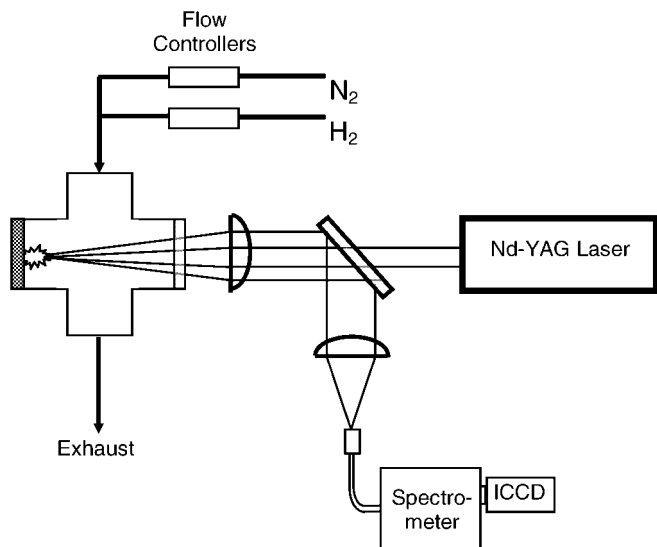


FIG. 1. Schematic of the LIBS system configured for surface breakdown, including the four-way sample cross, gas handling, and plasma emission collection optics.

for hydrogen detection. This may be due, in part, to the additional complications of using plasma spectroscopy with hydrogen species, namely, potential plasma ignition of hydrogen gas and spectral contamination by common atmospheric hydrogen contained in species such as water vapor. While LIBS has not been investigated for direct hydrogen leak detection, many laser-induced plasma studies have used various hydrogen lines for plasma diagnostics, notably Stark broadening measurements.<sup>9-14</sup>

## EXPERIMENTAL METHODS

The LIBS experimental system was developed using a 1064 nm Q-switched Nd:YAG laser operating with either 55 or 100 mJ pulse energy, 8 ns pulse width, and 2.5 Hz pulse repetition rate. The laser included a frequency doubling crystal that was detuned to minimize second harmonic generation; hence, the laser pulse was primarily 1064 nm with only trace amounts of 532 nm light. A schematic of the experimental apparatus is shown in Fig. 1. The unexpanded laser beam was focused using a 250 mm focal length plano-convex lens to form the sample spot. The focal spot was positioned within a four-way stainless steel cross-chamber by passing the laser beam through an optical window. Two methodologies were examined in the current study. In the first approach, a 55 mJ laser pulse was used to create the laser-induced plasma directly on a solid surface, namely, the stainless steel flange that sealed the vacuum cross opposite of the optical window. The four-way cross was positioned such that the focal spot of the laser was on the surface of the stainless steel flange. In the second method, a 100 mJ laser pulse was used to create the laser-induced breakdown directly in the sample gas stream at the laser focal spot, which was positioned such that the laser-induced plasma was formed in approximately the center of the cross. For both arrangements, the plasma emission was collected along the incident beam in a backward direction using the same primary focusing lens and separated using a 75 mm square pierced mirror. The collected light was

then focused into an optical fiber bundle coupled to a spectrometer (2400 grooves/mm grating, 0.12 nm optical resolution), and recorded with an intensified charge-coupled device (ICCD) array. The delay and integration width of the ICCD were set to optimize the hydrogen emission signal, with specific values reported below.

The two remaining flanges of the four-way cross were plumbed to a gas delivery and exhaust system. Mass flow controllers were used to deliver purified nitrogen and hydrogen (industrial grade) to the sample cross. The nitrogen was passed through a HEPA filter to remove any particulate contaminants, and both gases were passed through additional particle filters within the flow controllers. The nitrogen flow rate was fixed at 43.7 liters per minute (lpm), and the hydrogen flow rate was varied from zero to 16 lpm, with 0.04 lpm used as the minimum setting. To ensure precision and accuracy over the full range of hydrogen flow rates, two separate mass flow controllers were used. The sample cross was vented through tubing directly into a dedicated laboratory exhaust duct. It is noted that hydrogen is flammable from about 4 to 75% in air, and that a laser-induced plasma is a viable ignition source for a combustible mixture. To avoid flammability issues, all experiments involving hydrogen were performed in the four-way cross in the binary nitrogen/hydrogen mixtures, thereby eliminating the possibility of a flammable mixture.

Finally, it is noted that a preliminary series of experiments was performed in which various metals, including aluminum, copper, molybdenum, stainless steel, titanium, and tungsten, were analyzed as candidate substrate surfaces. During these experiments, the four-way cross was removed and measurements were performed by directly sparking on the candidate sample surfaces in ambient air. For these measurements, water vapor naturally present in the ambient air served as the hydrogen source.

## RESULTS AND DISCUSSION

To identify the best candidate material to serve as the target substrate for plasma formation, a range of materials was examined. Only metals were considered as candidate substrates due to the reduced laser pulse energy required for breakdown, which results from the higher electron densities and electron mobility and the relatively low ablation rates. This latter attribute of metals is important to limit substrate replacement in any actual detection device. Common materials with high electrical conductivity were examined, including copper and aluminum, in addition to materials with excellent surface hardness such as stainless steel and titanium. Finally, refractory materials characterized by high melting temperatures were examined, namely tungsten and molybdenum. For each material, a series of spectra were recorded using a fixed ICCD detector gate width of 2  $\mu$ s, while the detector delay with respect to the plasma-initiating laser pulse was varied between 2 and 12  $\mu$ s. The spectral window was centered on the 656.28 H $\alpha$  emission line, which was found to be the strongest hydrogen emission line of the Balmer series. As discussed above, ambient air was used as the source of hydrogen for this portion. The ambient air contained approximately 1.5% water vapor by volume, or 1000

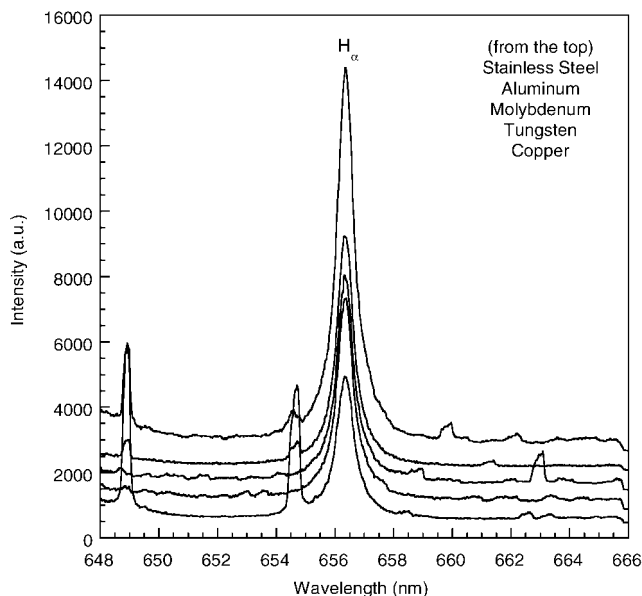


FIG. 2. LIBS spectra of candidate substrate materials recorded using a 55 mJ pulse directly in ambient air. All spectra have the same scale and are shifted vertically for clarity.

ppm of hydrogen by mass, based on the estimated relative humidity and temperature at the time of sampling.

The temporal measurements revealed an optimal hydrogen signal, as evaluated by the ratio of the hydrogen emission signal to the adjacent continuum emission signal, corresponding to detector delays from about 4 to 8  $\mu$ s. Representative spectra from the aluminum, copper, molybdenum, stainless steel, and tungsten substrates are shown in Fig. 2. The spectra corresponding to all five materials are characterized by strong atomic emission of the 656.28  $H_{\alpha}$  line. All spectra exhibit relatively clean continuum emission in the immediate region of the  $H_{\alpha}$  line, with the exception of two emission lines at 649.5 and 654.8 nm corresponding to the second-order lines originating from the 324.8 and 327.4 nm resonant Cu(I) lines. These lines are pronounced in the spectrum corresponding to the copper substrate and are of moderate intensity in the stainless steel and aluminum spectra due to trace elements in these two samples. The exact structure of the continuum emission is discussed in further detail below regarding Fig. 3. The titanium spectrum is not included in the figure. Although the titanium substrate produced a hydrogen signal comparable to the other materials, titanium is characterized by a number of atomic emission lines throughout the spectral region of interest. Based on the preliminary experiments, stainless steel was selected as the optimal material for the substrate surface due to its combination of yielding the greatest  $H_{\alpha}$  emission signal and a relatively clean continuum emission signal. In addition, the flange material for the four-way cross was stainless steel; hence, directly using the flange as the sample substrate eliminated any sample preparation and mounting issues.

The stainless steel substrate was used to investigate the overall sensitivity and signal linearity of the  $H_{\alpha}$  emission line. The stainless steel flange opposite the four-way-cross optical window was used as the stainless steel substrate. The sample cross was positioned with the laser

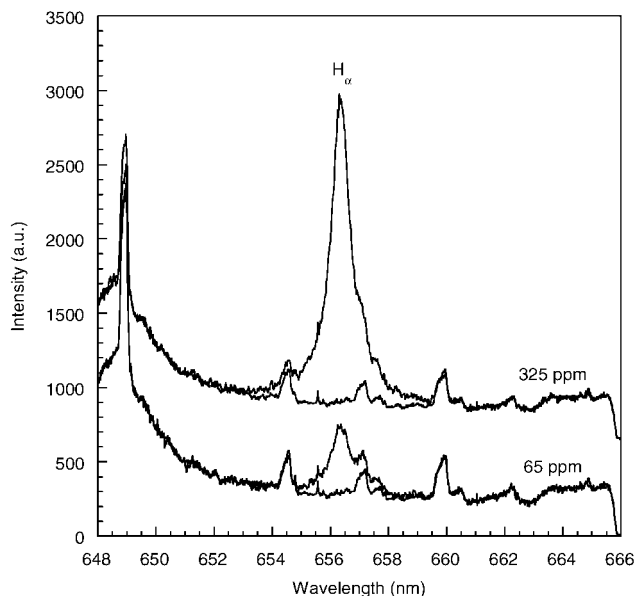


FIG. 3. LIBS spectra for hydrogen concentrations of 65 and 325 ppm and their corresponding scaled background spectra. The 325 ppm spectra have been shifted vertically for clarity.

focal spot on the stainless steel flange such that the laser-induced plasma was formed directly on the sample surface. A fixed detector delay of 4  $\mu$ s and a fixed gate width of 4  $\mu$ s were used for all subsequent experiments. The hydrogen flow rates were varied from zero to 16 lpm in a fixed flow of nitrogen. For each flow setting, beginning at zero hydrogen flow, a series of 50 LIBS spectra were collected and ensemble averaged. Following the final hydrogen flow rate, the system was flushed with nitrogen and a second pure nitrogen sequence was recorded.

The two ensemble-averaged spectra corresponding to nitrogen were averaged together for each experimental sequence to form the background spectrum. Subsequently, the background spectrum was scaled to fit the spectrum recorded for each hydrogen flow rate. The scaling was done using a fixed multiplier based on the average ratio of the hydrogen spectrum to the blank spectrum as determined using spectral regions on each side of the  $H_{\alpha}$  line. Representative hydrogen spectra and the scaled background spectra are shown in Fig. 3 corresponding to hydrogen concentrations of 65 and 325 ppm (mass), or to hydrogen flow rates of 0.04 and 0.2 lpm, respectively. The background spectra corresponding to pure nitrogen do reveal some structure near the hydrogen emission line. To quantify the hydrogen emission line, the full width of the  $H_{\alpha}$  line was integrated, as was the full width of the corresponding scaled background spectrum. The integrated background signal was subtracted from the integrated hydrogen signal, yielding the integrated peak area of the  $H_{\alpha}$  line. To normalize for variations in absolute signal strength (i.e., reduced detector binning at higher hydrogen concentrations), the integrated hydrogen signal was normalized by the integrated background signal (i.e., continuum). The resulting peak-to-base (P/B) ratio is widely used for LIBS analysis, and it functions to enhance precision by scaling the fluctuations in absolute plasma emission that are characteristic of the LIBS technique.<sup>15</sup> To demonstrate the excellent scaling and back-

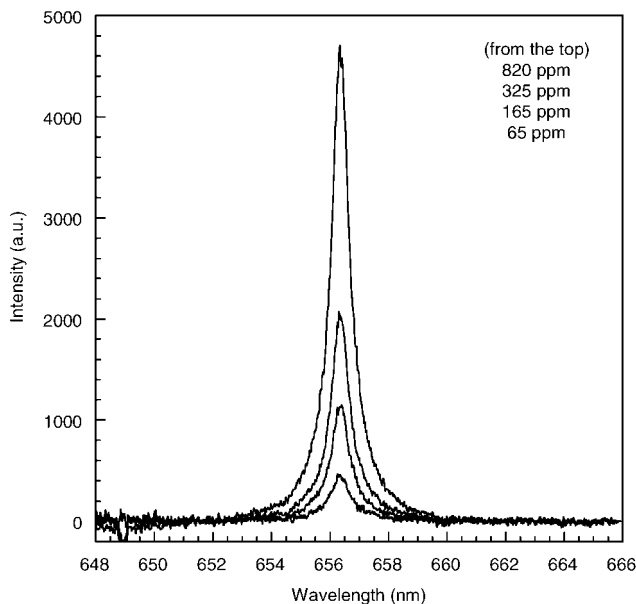


FIG. 4. Background-subtracted LIBS spectra corresponding to different hydrogen concentrations in a balance of nitrogen. All spectra have the same scale.

ground subtraction results, background-subtracted spectra are presented in Fig. 4 for hydrogen concentrations of 65, 165, 325, and 820 ppm.

The P/B ratios corresponding to the  $H_{\alpha}$  line are plotted in Fig. 5 as a function of hydrogen concentration (by volume) for the stainless steel substrate experiments up to a concentration of 4.4%, which corresponds to 3260 ppm of hydrogen on a mass basis. The error bars represent plus or minus one full standard deviation based on two to three trials, with each trial generating multiple 50-shot ensemble-averaged spectra. The hydrogen signal is very linear ( $R > 0.999$ ) up to a concentration of about 1.1% (820 ppm by mass), after which the signal response departs somewhat from the linear response, possibly due to slight self-absorption effects that are characteristic of the curve of growth for atomic emission. The slope of the linear response regime was used to calculate the detection limit by extrapolating the calibration curve to a value such that the P/B ratio was three times the value of the integrated full-width root mean square (rms) noise. The rms noise was calculated from the scaled background spectrum corresponding to the minimum recorded hydrogen concentration of 65 ppm (mass). The detection limit was calculated for each of three experiments performed at this minimum concentration and then averaged. This procedure yielded a hydrogen detection limit of 15 ppm on a mass basis. This detection limit corresponds to about one-fourth of the minimum hydrogen concentration actually measured, which was determined by the lowest practical flow rate of the hydrogen flow controller.

The above procedures were repeated for the second methodology, namely the formation of the plasma directly in the gaseous sample stream without the aid of any solid surface. As discussed above, the laser energy was increased to 100 mJ per pulse to generate consistent breakdown in the purely gas-phase sample stream. The LIBS spectral data were analyzed as described above, and the resulting  $H_{\alpha}$  line P/B ratios are plotted in Fig. 5 along

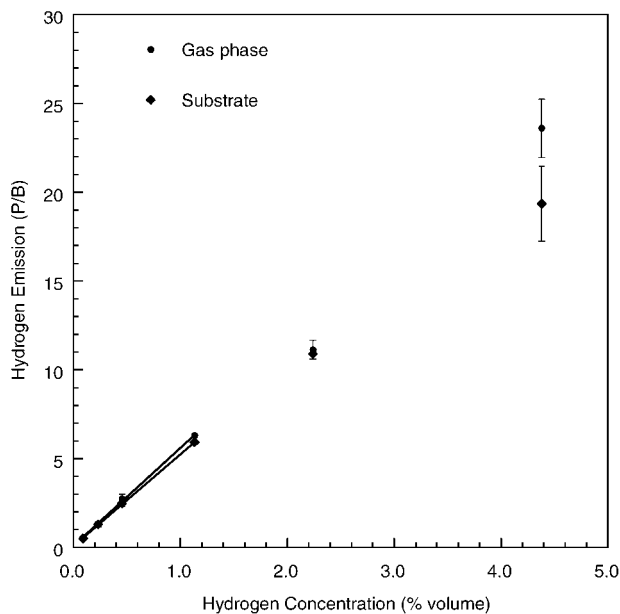


FIG. 5.  $H_{\alpha}$  emission as a function of hydrogen concentration for plasma formation on the stainless steel substrate, and for plasma formation directly in the sample gas stream.

with the previous results. As before, the hydrogen signal is very linear ( $R > 0.999$ ) up to a concentration of about 1.1% (820 ppm by mass), after which the signal response again departs from the linear response. For the purely gas-phase plasma, the calculated hydrogen detection limit is 23 ppm (mass). This detection limit is remarkably consistent with the result determined for the stainless steel generated plasma (note the similar slopes in Fig. 5), which suggests a similar plasma in both cases despite the differences in breakdown initiation. It is noted that the plasma generated on the solid surface departs somewhat more from a linear response than the gas-phase generated plasma, which may reflect a plasma size effect due to the reduced laser pulse energy of the former.

A comparison of the spectral line widths between the two methodologies was made to determine if the resulting plasmas were comparable in electron density. Assuming Stark broadening to be the dominant broadening mechanism for the  $H_{\alpha}$  emission line (656.28 nm), the plasma electron density can be extracted using the full width at half-maximum (FWHM) spectral line width, in a manner reported by Griem.<sup>10,11</sup> More recent methods of calculating electron densities that incorporate updated broadening constants and ion dynamics<sup>13,14</sup> are not addressed, as the currently reported electron densities are primarily for relative comparison purposes. Using the FWHM, the electron densities were calculated for both the gas phase and stainless steel generated plasmas at three intermediate hydrogen concentrations. An average plasma temperature of 20000 K was used for all calculations. Calculation of electron densities via Stark broadening is rather insensitive to the assumed plasma temperature. To assess the uncertainty in the present calculations, the maximum error was evaluated using an uncertainty of  $\pm 10000$  K, which is represented by the error bars. The electron densities calculated for both the solid surface and gas-phase plasmas are shown in Fig. 6 as a function of hydrogen gas concentration. As shown in Fig. 6, the electron den-

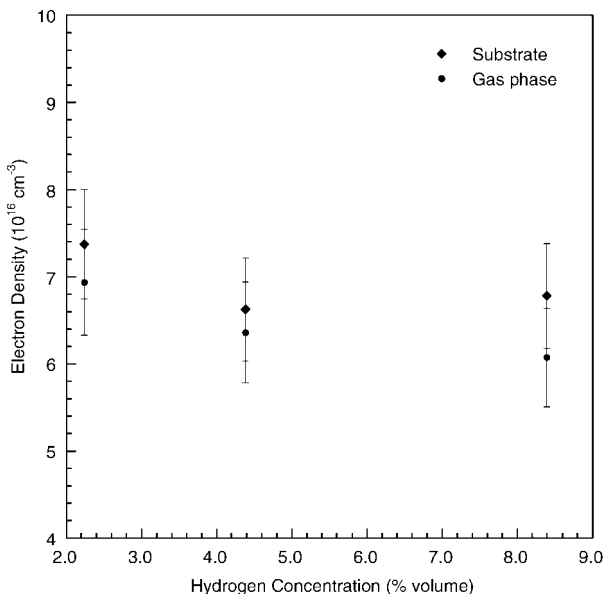


FIG. 6. Plasma free-electron densities at three sample hydrogen concentrations for the stainless steel substrate and gas-phase generated plasmas. The electron densities were calculated based on Stark broadening observed in the  $H_{\alpha}$  emission line.

sities of the two plasmas are comparable, falling within the experimental uncertainty, at each of the three sample concentrations examined. However, a slightly higher electron density is observed in all cases for the plasma generated on the stainless steel substrate, most likely due to the higher electron density of the metal substrate prior to breakdown. The comparable electron densities verify the similarity of the two plasmas, thus supporting the consistent detection limits observed.

While the data presented in Fig. 5 are limited to concentrations near the regime characterized by a highly linear response to facilitate calculation of the detection limits, measurements were extended to greater hydrogen concentrations. The P/B ratios are presented in Fig. 7 for the gas-phase initiated breakdown measurements up to a hydrogen concentration of 26.8%, which corresponds to a mass-based hydrogen concentration of 25 500 ppm. As seen in Fig. 7, linear behavior on the log-log plot is observed throughout the range of hydrogen concentrations. The linearity observed in the curve of growth illustrates that emission in this concentration regime is not appreciably affected by optical depth and thus there is no significant self-absorption mechanism affecting the analyte signal.<sup>16</sup> Overall, the data presented in Figs. 5 and 7 demonstrate the excellent analyte response of hydrogen to the LIBS technique.

## CONCLUSION

In summary, the current study demonstrates that detection of hydrogen can be made using the LIBS technique down to mass concentrations of about 20 ppm. Both of the methodologies yielded similar results; however, the solid surface initiated breakdown was accomplished at one-half of the pulse energy required for breakdown in the pure gas phase. The results with the 55 mJ laser are particularly encouraging, in that several compact lasers are commercially available in that energy range.

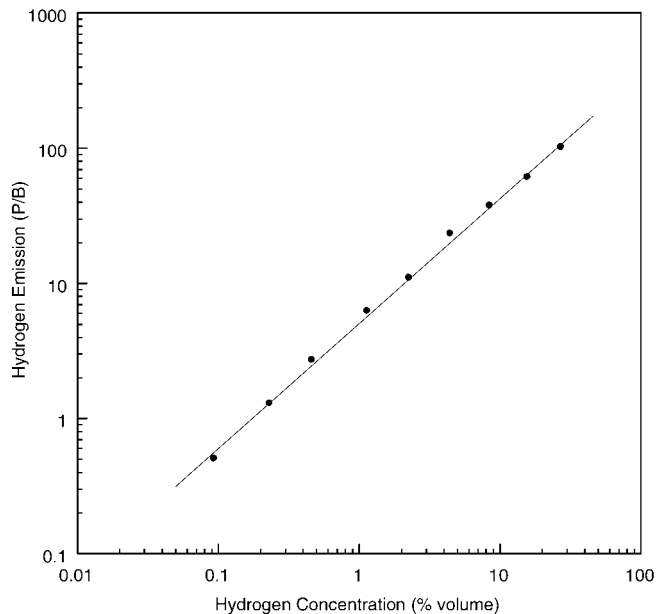


FIG. 7.  $H_{\alpha}$  emission as a function of hydrogen concentration for plasma formation directly in the sample gas stream. The solid line has been added for clarity.

Noting that water vapor from ambient air was an excellent source of hydrogen emission, the discrimination of atomic hydrogen signals from such non- $H_2$  sources may be an issue for implementation of hydrogen leak sensors. Several solutions are apparent, including the removal of water vapor by passing the sample stream through a cold trap (e.g., liquid nitrogen) prior to entering the LIBS chamber, and multi-species analysis algorithms that make use of argon and carbon (from carbon dioxide) emission signals (both present in ambient air) to aid in the discrimination of ambient-air-derived hydrogen ( $H_2O$ ) and true hydrogen gas ( $H_2$ ). For applications like the space shuttle program, existing gas sampling lines could be simultaneously fed to a LIBS sample chamber for additional analysis. Finally, safety considerations should be explored with any implementation of a LIBS-based hydrogen sensing system. For example, the LIBS sample cell should be of rigid construction and contain a minimum gas sample volume with all gas exchange passed through porous (i.e., sintered) filters such that all spatial dimensions are well below the flame quenching dimensions for all possible gas mixtures, thereby isolating any ignition sources and explosion potential within the sample cell. With these considerations addressed, a LIBS-based hydrogen sensing system is concluded to be a viable option for real-time hydrogen leak detection.

## ACKNOWLEDGMENTS

This work was supported in part by the NASA Hydrogen Research for Spaceport and Space Based Applications, GRC # NAG3-2930, and by the NASA Graduate Student Researchers Program (Allen Ball). The authors acknowledge Dr. Robert Youngquist (NASA KSC) for encouragement to pursue this work, as well as for useful discussions.

1. T. P. Griffin, G. S. Breznik, C. A. Mizell, W. R. Helms, G. R. Naylor, and W. D. Haskell, *Trends Anal. Chem.* **21**, 488 (2002).
2. L. Dudragne, Ph. Adam, and J. Amouroux, *Appl. Spectrosc.* **52**, 1321 (1998).
3. C. K. Williamson, R. G. Daniel, K. L. McNeisby, and A. Miziolek, *Anal. Chem.* **70**, 1186 (1998).

4. M. Tran, B. W. Smith, D. W. Hahn, and J. D. Winefordner, *Appl. Spectrosc.* **55**, 1455 (2001).
5. J. B. Simeonsson and A. W. Miziolek, *Appl. Phys. B* **59**, 1 (1994).
6. J. B. Simeonsson and A. W. Miziolek, *Appl. Opt.* **32**, 939 (1993).
7. R. J. Nordstrom, *Appl. Spectrosc.* **49**, 1490 (1995).
8. F. Ferioli, P. Puzinauskas, and S. G. Buckley, *Appl. Spectrosc.* **57**, 1183 (2003).
9. C. Parigger, D. H. Plemmons, and J. W. L. Lewis, *Appl. Opt.* **34**, 3325 (1995).
10. S. Itoh, M. Shinoda, K. Kitagawa, N. Arai, Y. I. Lee, D. Q. Zhao, and H. Yamashita, *Microchem. J.* **70**, 143 (2001).
11. H. R. Griem, *Spectral Line Broadening by Plasmas* (Academic Press, New York, 1974).
12. V. Hohreiter, J. E. Carranza, and D. W. Hahn, *Spectrochim. Acta, Part B* **59**, 327 (2004).
13. M. A. Gigosos and V. Cardenoso, *J. Phys. B: At., Mol., Opt. Phys.* **29**, 4795 (1996).
14. E. Oks, *J. Quant. Spectrosc. Radiat. Trans.* **65**, 405 (2000).
15. J. E. Carranza and D. W. Hahn, *Spectrochim. Acta, Part B* **57**, 779 (2002).
16. J. A. Aguilera, J. Bengoechea, and C. Aragon, *Spectrochim. Acta, Part B* **58**, 221 (2003).